Resilient composite of silicone and foamed tin as a new material for electrical and thermal contacts

MINGGUANG ZHU and D.D.L. CHUNG

(State University of New York at Buffalo, USA)

Silicone-infiltrated tin foam containing 14 volume % metal is a new composite material that is resilient up to a compressive stress of 2 MPa and a strain of 13%. Its volume electrical resistivity is 5×10^{-4} Ω cm and remains below 1×10^{-3} Ω cm up to 1700 compressive loading cycles (0.075 MPa). Its contact resistivity (with copper) decreases with pressure and levels off at 0.22 Ω cm^2 at a pressure of 0.07 MPa. Beyond 1000 compressive loading cycles (0.08 MPa), the contact resistivity rises, reaching 0.48 Ω cm^2 at 1700 cycles. The thermal expansion coefficient is 215×10^{-6}°C^{-1} at 45°C, compared with a value of 282×10^{-6}°C^{-1} for silicone. This composite is attractive as a material for electrical and thermal contacts in electronic packages. Compared with silicone-infiltrated tin foam, silicone-infiltrated tin–lead foam exhibits a lower volume electrical resistivity, a lower contact resistivity (with copper) and a higher fatigue resistance, but it is resilient only up to a compressive stress of 0.4 MPa and a strain of 0.8%. The bonding between silicone and tin is stronger than that between silicone and tin–lead.

Key words: *composite materials; electrical properties; mechanical properties; silicone-infiltrated tin foam; silicone-infiltrated tin–lead foam*

Separable electrical connectors are important for electronic packaging in the context of pad-to-pad connections as well as pin-in-socket type connections. They are attractive because they do not require heating or defluxing (as in the case of soldered joints) and they are convenient for rework, repair and maintenance. The material for separable electrical connectors requires a low electrical resistivity, good corrosion resistance (to minimize the contact resistivity) and preferably resilience as well (also to minimize the contact resistivity).

Thermal interface or thermal contact materials are also important for electronic packaging to allow effective heat dissipation, which is critical for high-density electronic packages. Such materials require a high thermal conductivity and good corrosion resistance as well as resilience.

Conducting elastomers are elastomers filled with an electrically and thermally conducting material in the form of particles, wires, layers, strips or springs. For elastomers filled with conducting particles, because the conducting particles are not continuous, the electrical resistivity of such a composite is typically above 10^{-2} Ω cm and the thermal conductivity of such a composite is much lower than those of metals. For elastomers filled with continuous and conducting layers, strips, wires or springs, the electrical resistivity can be lower than that of the particle-filled counterpart, but the relatively small interfacial area between the filler and the elastomer matrix makes the bonding force between the filler and matrix relatively weak and the geometry of the filler and the matrix does not allow much, if any, coherence due to mechanical interlocking.

Instead of using conducting particles, wires, layers, strips or springs in an elastomer to provide a conducting and resilient composite, we have used foamed metal (an interconnected three-dimensional metal framework) in an elastomer to provide a resilient composite that has an electrical resistivity of 5×10^{-4} Ω cm. Because the metal and the elastomer are in the form of two interpenetrating continuous frameworks, the two phases interlock. In order for the composite to be resilient, the metal must be soft and ductile. Tin was therefore chosen. The elastomer used was silicone.

Foamed metals may be prepared by casting, metallic deposition, powder metallurgy or sputter deposition[1]. In particular, the casting method may involve foaming in melts, casting around granules, investment casting or incorporating hollow spheres in melts[1]. In this work, foamed tin was prepared by casting around sodium chloride granules, which are soluble in water and can

0010-4361/91/030219-08 © 1991 Butterworth-Heinemann Ltd

thus be leached out to leave a foamed metal. Foamed aluminium of porosity 65–70 volume % (vol %) had previously been made by similar methods, using granules of size 1–5 mm[2,3]. In this work, foamed tin of porosity 86 vol % was prepared by using NaCl granules of size 0.3 mm.

After infiltrating the foamed tin with silicone and allowing the silicone to cure, a new composite material was obtained which exhibits attractive electrical and mechanical properties.

In addition to tin, a tin–lead alloy containing 37 weight % (wt %) Pb (a common solder alloy) was also used in this work. The resulting silicone composite with tin–lead was superior to that with tin in the electrical properties, but was inferior to the tin counterpart in the mechanical properties. The tin–lead composite was resilient up to a compressive stress of 0.4 MPa and a strain of 0.8%, whereas the tin composite was resilient up to a compressive stress of 2 MPa and a strain of 13%. The poor mechanical properties of the tin–lead composite were due to the less ductile nature of tin–lead compared with tin and the poor bonding between tin–lead and silicone.

COMPOSITE PREPARATION

Preparation of foamed metals

Two kinds of alloys were used: pure tin and tin–lead containing 37 wt % Pb. They were both in ingot form.

Two types of NaCl granules were used: table salt and mineral rock salt (Halite Melting Crystals, Sterling). The as-received table salt is shown in Fig. 1; it was in the form of cubes with sharp corners; the particle size was typically 0.3 mm and it had a narrow size distribution. Before use, the table salt was ball-milled to make the corners of each cube more round. The ball-milled table salt is shown in Fig. 2 at two different magnifications. Before use, the rock salt was crushed into granules of irregular shape; the particle size of the crushed rock salt was in the range from 0.71 to 1.00 mm and the size distribution was broader than that of the table salt. The crushed rock salt is shown in Fig. 3.

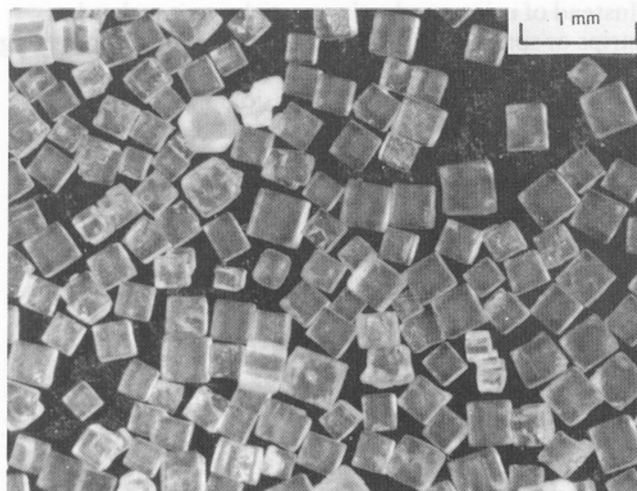

Fig. 1 Optical micrograph of as-received table salt

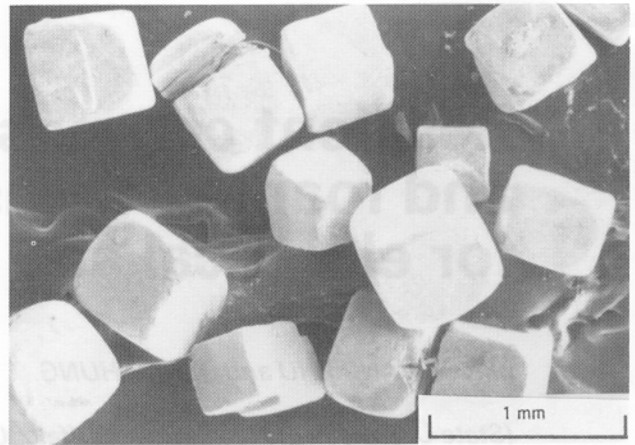

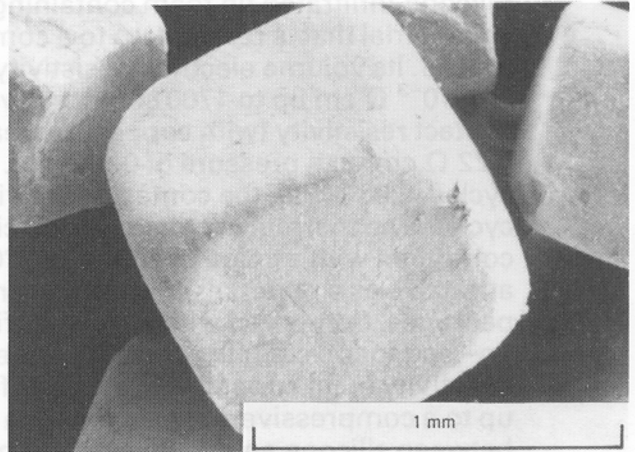

Fig. 2 SEM micrographs of ball-milled table salt at two different magnifications

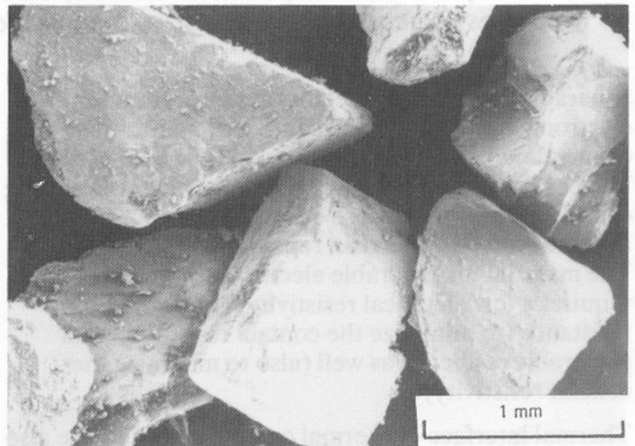

Fig. 3 SEM micrograph of crushed rock salt

An inorganic, water-soluble, temperature-resistant binder was used to bind the salt particles together.

Salt and the binder were mixed in the ratio of 100 to 6 and then pressed at 4.1–6.9 MPa and room temperature in a steel mould to form a salt preform. Then the preform was dried in air at 200°C for 2 h. After that, the preform was allowed to cool. Subsequently, additional binder was applied to the preform and then the preform was dried at 200–250°C for 2–3 h.

The preform was placed at the bottom of a steel mould, which was then heated to 130–150°C so that the

preform also reached this temperature. Liquid metal (Sn or Sn–Pb) at 280–320°C was then poured into the mould and immediately a pressure of 41–83 MPa was applied through a ram to the liquid metal so as to infiltrate the preform with the liquid metal. This process (known as squeeze casting) resulted in a salt–metal composite in which both the salt and metal were continuous phases. After this, the salt–metal composite was immersed in water in order to wash away the salt by dissolution. After washing, a foamed metal was obtained.

Preparation of composites of foamed metals and silicone

The silicone was a general purpose sealant (100% silicone rubber), manufactured by Dow Corning.

A layer of porous material was first placed at the bottom of a steel mould, foamed metal was placed on top of the porous material and then silicone was placed on top of the foamed metal. Next a pressure of 41–83 MPa was applied to the silicone through a ram in order to infiltrate the foamed metal with the silicone, while air from the foamed metal was displaced to the porous material underneath the foamed metal in the mould. After this, the composite of foamed metal and silicone was removed from the mould and left at room temperature for 24 h in order to cure the silicone.

Fig. 4 shows scanning electron microscope (SEM) photographs at three different magnifications of foamed tin made using table salt. Because of the cubic shape of the table salt granules, the foamed metal had a microstructure which exhibited features with sharp corners. Because the connection between adjacent salt granules was narrow spatially, the morphology of the foamed metal contained features that were thin and flaky, as most clearly shown by the bottom photograph with the highest magnification in Fig. 4.

Composites made using table salt were labelled A and those using rock salt were labelled B. The following materials were prepared: Sn/silicone A, Sn–Pb/silicone A and Sn–Pb/silicone B. Comparison between Sn/silicone A and Sn–Pb/silicone A reveals the difference between Sn and Sn–Pb composites, whereas the effect of using the two different types of salt is found by comparison between Sn–Pb/silicone A and Sn–Pb/silicone B.

COMPOSITE CHARACTERIZATION

The foamed metal/silicone composites were characterized by compression testing, metallography, fractography, volume electrical resistivity measurement, contact electrical resistivity measurement and thermal expansion measurement.

Compression testing

Compression testing was performed using a Vishay Bench Top Testing Machine (Model BT-1000). Fig. 5 shows compressive stress/strain curves of Sn/silicone A and silicone. The left-hand curve in Fig. 5 exhibits a discontinuous change in slope at a stress of about

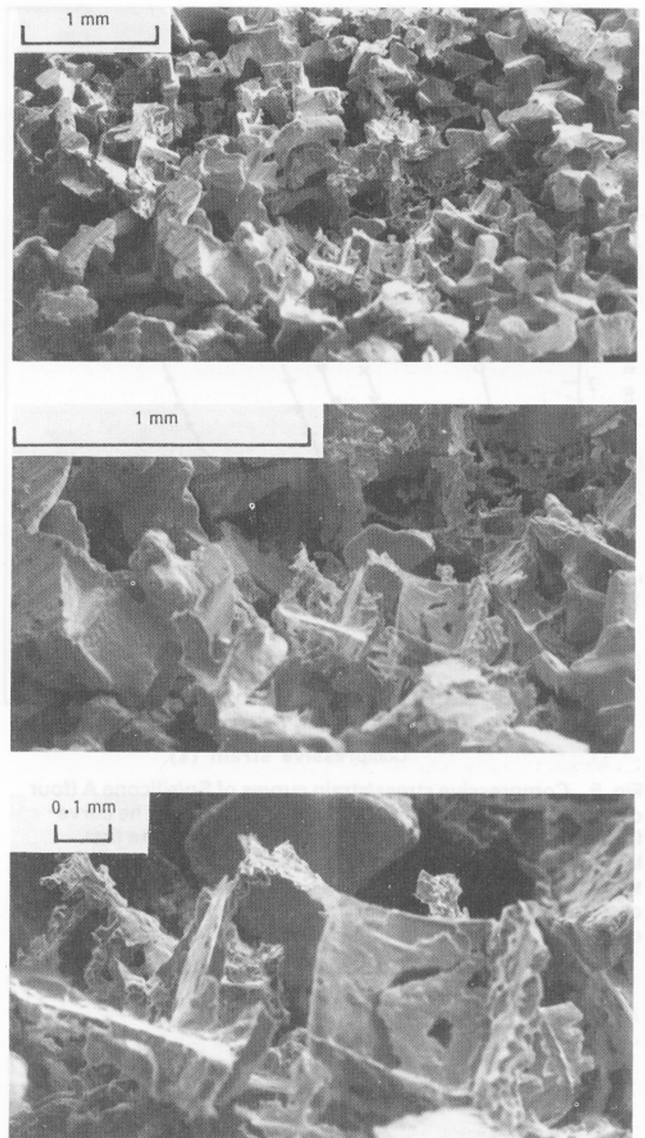

Fig. 4 SEM micrographs at three different magnifications of foamed tin made using table salt

2 MPa; it is the stress/strain curve of Sn/silicone A during the first loading cycle. As long as the applied compressive stress did not exceed that corresponding to the discontinuous change in slope, the deformation was totally reversible and all subsequent loading cycles exhibited exactly the same stress/strain curve. However, if the applied compressive stress exceeded that corresponding to the discontinuous change in slope, subsequent loading cycles followed smooth curves (the three shown in the middle of Fig. 5 are for the second, fourth and fifth cycles), which resemble in shape the stress/strain curve of silicone, the right-hand curve in Fig. 5. The permanent offset after the first cycle (carried out beyond the point of discontinuous change in slope) was 3%, and was 4% after all subsequent cycles. Hence, Sn/silicone A was resilient up to a compressive stress of 2 MPa and a corresponding strain of 13%.

Fig. 6 shows the compressive stress/strain curve of Sn–Pb/silicone B during the first loading cycle compared with that of silicone. The corresponding

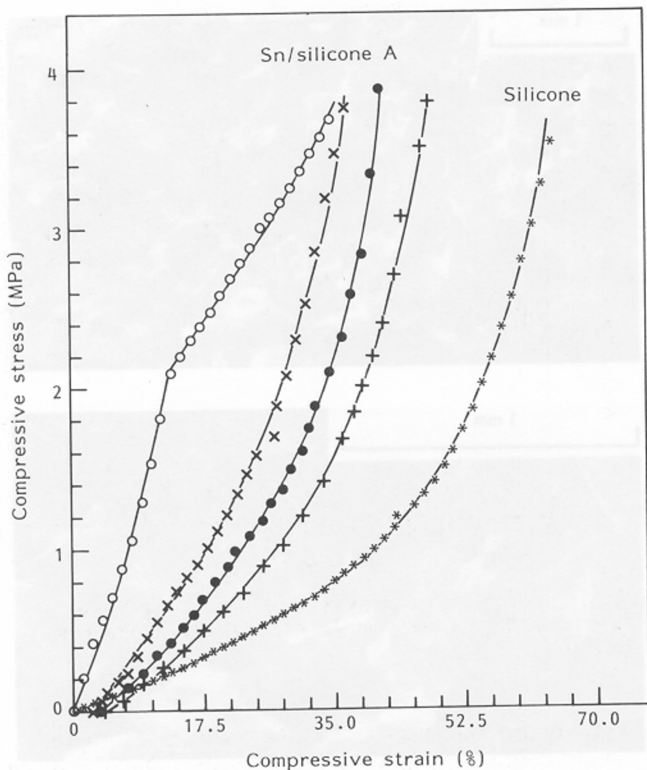

Fig. 5 Compressive stress/strain curves of Sn/silicone A (four curves at the left) and silicone (right-hand curve). The curve furthest to the left is that for Sn/silicone A during the first loading cycle. The middle three smooth curves are for the second, fourth and fifth cycles of Sn/silicone A, such that the corresponding first cycle was carried out beyond the point of discontinuous change in slope (at about 2 MPa)

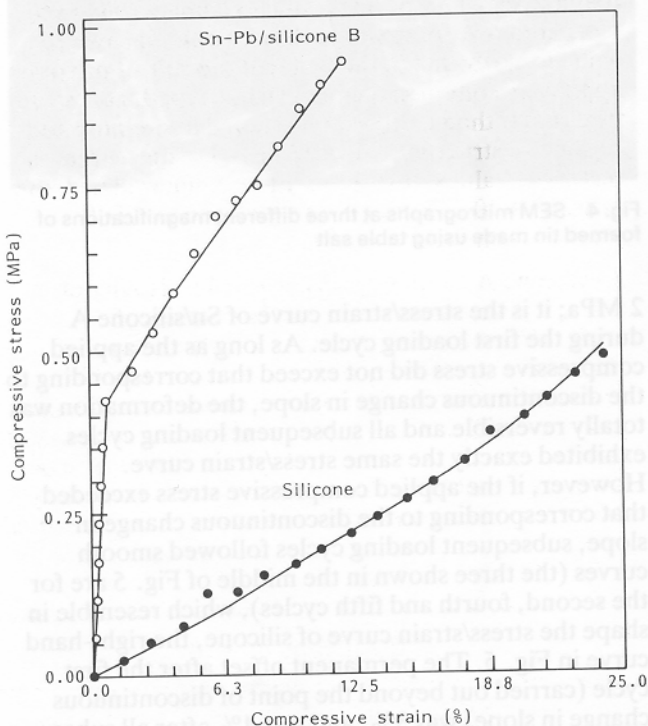

Fig. 6 Compressive stress/strain curves of Sn–Pb/silicone B and silicone during the first loading cycle

curve for Sn–Pb/silicone A (not shown) is similar to but slightly beneath that of Sn–Pb/silicone B. As long as the compressive stress did not exceed 0.4 MPa, which corresponds to that of the discontinuous change in slope of the stress/strain curve, the deformation was totally reversible and all subsequent loading cycles exhibited exactly the same stress/strain curve. However, when this stress level was exceeded, cracking of the Sn–Pb was observed and all subsequent cycles exhibited a stress/strain curve that exactly overlapped that of silicone itself. The cracked surfaces of Sn–Pb cut the silicone upon further compression. Hence, Sn–Pb/silicone B was resilient up to a low compressive stress of 0.4 MPa and a corresponding strain of 0.8% and fracture began when this stress level was exceeded. Sn–Pb/silicone A was resilient up to an even lower compressive stress of 0.33 MPa and a corresponding strain of 0.66%.

Metallography

The composites were polished using sand paper. Subsequent examination by SEM yielded the photographs of Fig. 7. For Sn/silicone A (Fig. 7(a)), the polishing removed a part of the tin at the surface; the interface between tin (bright regions in the photograph) and silicone was clearly seen. For Sn–Pb/silicone B (Fig. 7(b)), the polishing removed a part of the silicone such that the fracture occurred mostly at the interface between Sn–Pb (bright regions in the photograph) and silicone.

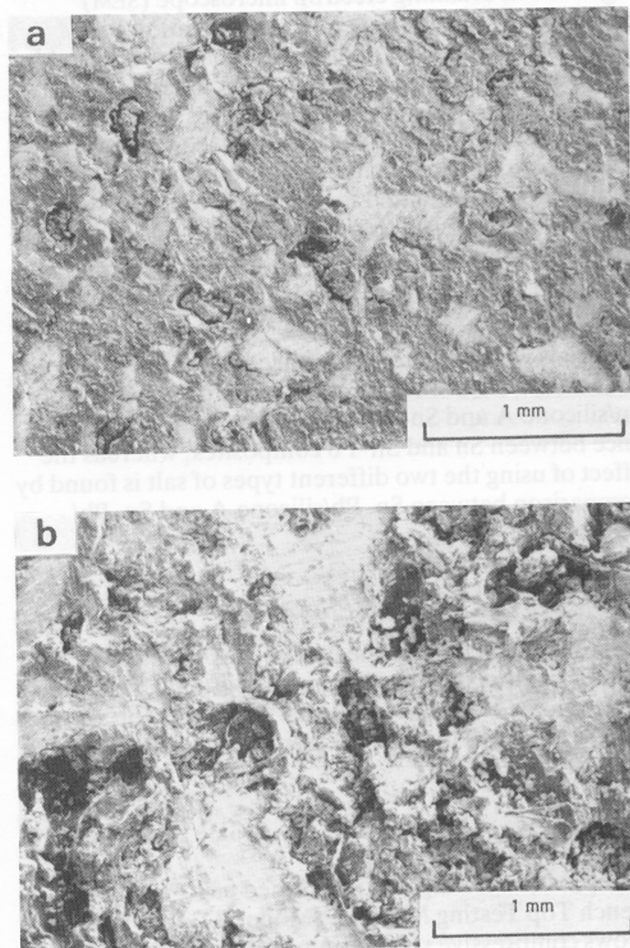

Fig. 7 SEM micrographs of polished sections of: (a) Sn/silicone A; and (b) Sn–Pb/silicone B

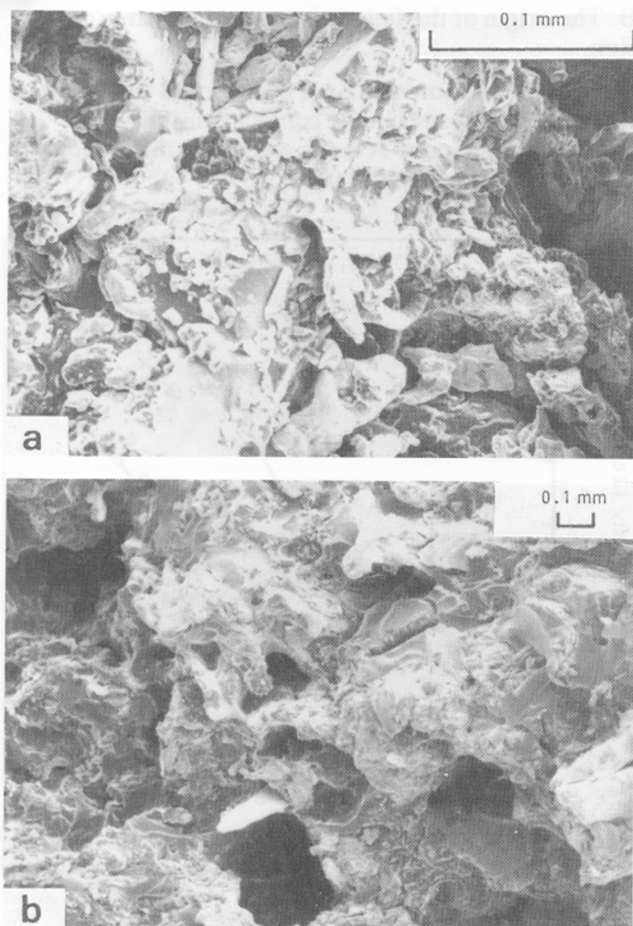

Fig. 8 SEM micrographs of the tensile fracture surfaces of: (a) Sn/silicone A; and (b) Sn–Pb/silicone B

Fractography

Tensile fracture surfaces of the composites were examined by SEM. For Sn/silicone A (Fig. 8(a)), the fracture surface showed that the silicone had been torn to fracture and an appreciable amount of tin remained on the fracture surface. For the fracture surface of Sn–Pb/silicone B (Fig. 8(b)), most of the Sn–Pb had been pulled out, leaving deep cavities surrounded by silicone. Thus, the bonding between the metal and the silicone was much better for Sn than for Sn–Pb.

Volume electrical resistivity

The four-probe method was used to measure the volume electrical resistivity. Silver paint was used for making the four electrical contacts on each sample. Table 1 shows the experimental results. The measured resistivity values are higher than those calculated using the rule of mixtures. The difference between the measured and calculated values is particularly large for Sn/silicone A. This is attributed to the physical damage that might be done to the foamed tin during the silicone infiltration. The foamed Sn–Pb was stiffer than the foamed Sn, so it was less prone to damage. That the measured resistivity was higher than the calculated value is partly due to the fact that the rule of mixtures applies to a one-dimensional aligned conductor structure rather than a three-dimensional interconnected conductor structure. Nevertheless, the measured resistivity values were all very low compared with the value of $\geqslant 10^{-2}$ Ω cm for a typical commercially available conducting silicone.

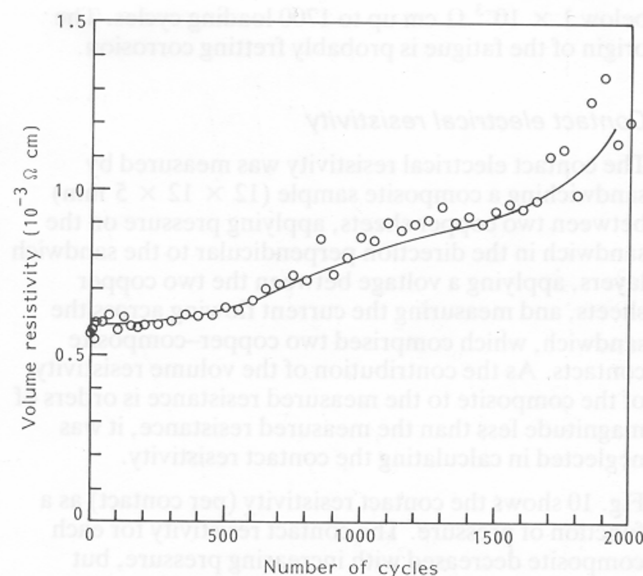

Fig. 9 Volume electrical resistivity of Sn/silicone A as a function of the number of cycles of compressive loading at 0.075 MPa

Sn/silicone A exhibiting an electrical resistivity of 6×10^{-4} Ω cm was compressed to a stress of 0.075 MPa (below the level for the discontinuous change in slope and equal to the pressure for the contact resistivity with copper to attain the minimum, as shown in Fig. 10). Fig. 9 shows the volume resistivity as a function of the number of cycles of loading under compression at 0.075 MPa. The objective is to study the fatigue resistance. The volume resistivity remained

Table 1. Volume electrical resistivity

Material	Metal content (vol %)	Resistivity (Ω cm) Measured	Resistivity (Ω cm) Calculated
Sn/silicone A	14	4.4×10^{-4}	7.1×10^{-5}*
Sn–Pb/silicone B	15	1.9×10^{-4}	1.0×10^{-4}†
Sn–Pb/silicone A	15	2.3×10^{-4}	1.0×10^{-4}†

* Based on the rule of mixtures using a resistivity of 1.0×10^{-5} Ω cm for Sn
† Based on the rule of mixtures using a resistivity of 1.5×10^{-5} Ω cm for Sn–Pb

below 1×10^{-3} Ω cm up to 1700 loading cycles. The origin of the fatigue is probably fretting corrosion.

Contact electrical resistivity

The contact electrical resistivity was measured by sandwiching a composite sample (12 × 12 × 5 mm) between two copper sheets, applying pressure on the sandwich in the direction perpendicular to the sandwich layers, applying a voltage between the two copper sheets, and measuring the current flowing across the sandwich, which comprised two copper–composite contacts. As the contribution of the volume resistivity of the composite to the measured resistance is orders of magnitude less than the measured resistance, it was neglected in calculating the contact resistivity.

Fig. 10 shows the contact resistivity (per contact) as a function of pressure. The contact resistivity for each composite decreased with increasing pressure, but levelled off at about 0.075 MPa. The levelled-off value was higher for Sn/silicone A than for Sn–Pb/silicone A or Sn–Pb/silicone B because the Sn/silicone A surface had a part of the soft tin removed from the surface, as caused by the cutting of the composite during the specimen preparation, whereas the Sn–Pb/silicone surface had a part of the silicone removed from the surface. The levelled-off value of the contact resistivity was lower for Sn–Pb/silicone B than for Sn–Pb/silicone A.

Fig. 11 shows the contact resistivity as a function of the number of cycles of loading under compression at 0.0827 MPa. The objective is to study the fatigue resistance. Low contact resistivity was maintained up to ~ 800 cycles for Sn/silicone A, ~ 1000 cycles for Sn–Pb/silicone A and ~ 1500 cycles for Sn–Pb/silicone B. The origin of the fatigue is probably fretting corrosion.

Figs 10 and 11 show that Sn–Pb/silicone B is the best of the three composites in the contact resistivity. Although Sn/silicone A is the worst, the differences among the three are not large.

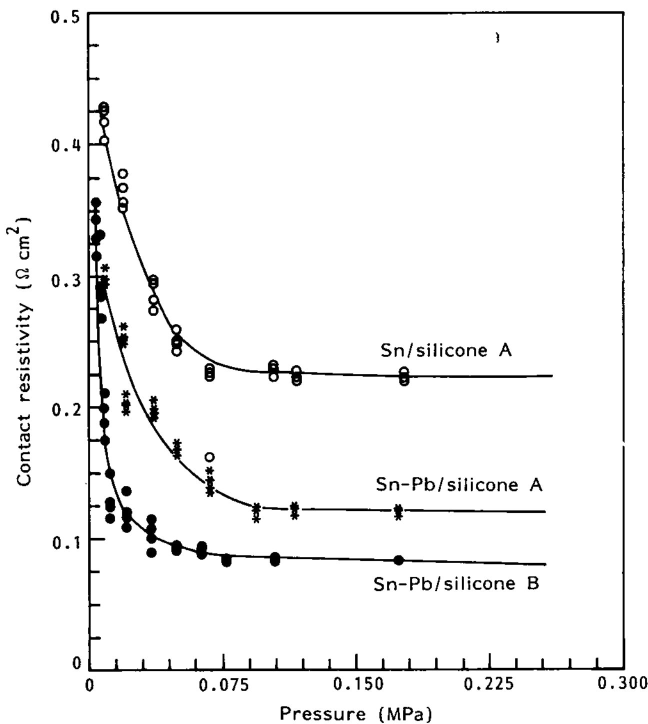

Fig. 10 Contact electrical resistivity of Sn/silicone A, Sn–Pb/silicone A and Sn–Pb/silicone B, each in contact with copper, as a function of pressure

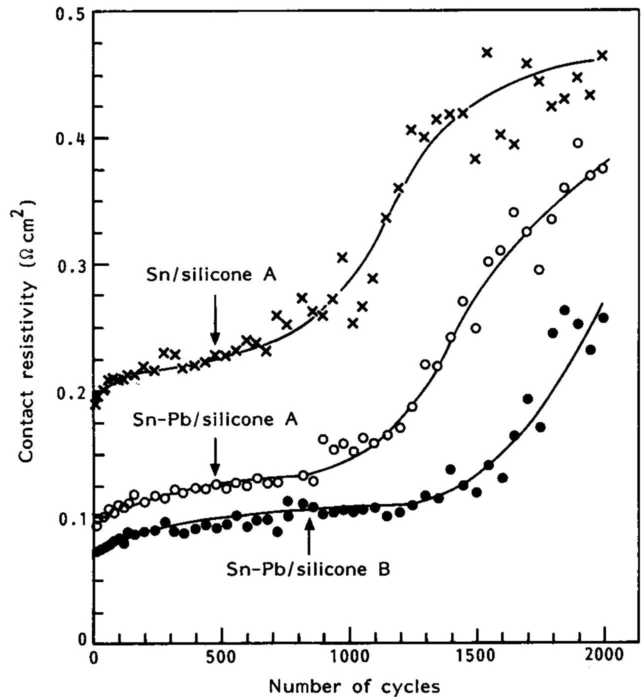

Fig. 11 Contact electrical resistivity of Sn/silicone A, Sn–Pb/silicone A and Sn–Pb/silicone B, each in contact with copper, as a function of the number of cycles of compressive loading at 0.0827 MPa

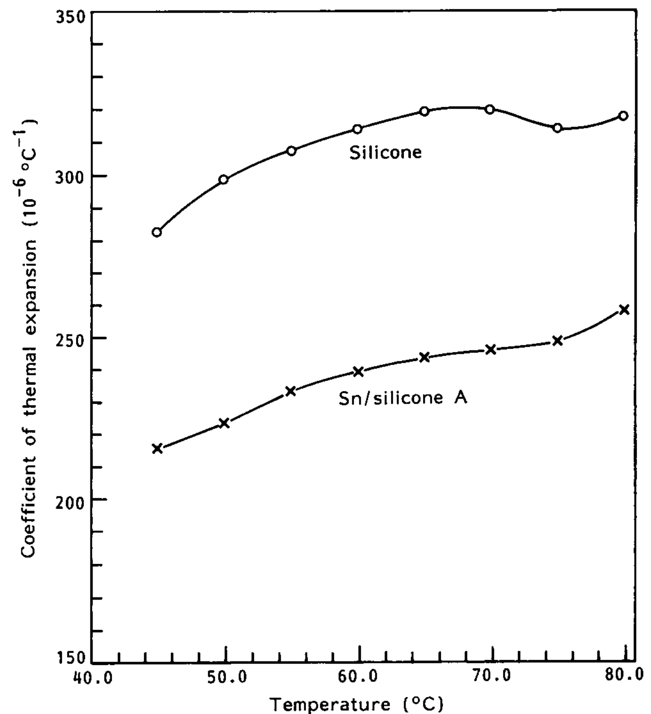

Fig. 12 Coefficient of thermal expansion as a function of temperature of silicone and Sn/silicone A

Thermal expansion

A Mettler TMA–40 thermal mechanical analyser was used to measure the coefficient of thermal expansion (CTE) at various temperatures. Fig. 12 shows the CTE of silicone and Sn/silicone A. That the CTE of Sn/silicone A was much lower than that of silicone itself shows that the bonding between Sn and silicone is good, in agreement with the results of metallography and fractography. The reduced CTE of Sn/silicone A is attractive for the use of this composite in electronic packaging.

DISCUSSION

This paper provides a new family of composites, i.e., composites of an elastomer and a foamed metal such that both the elastomer and the metal are continuous phases and the two phases mechanically interlock with one another. By using a soft and ductile metal for the foamed metal, we obtained a novel composite which is resilient (like an elastomer) and electrically and thermally conducting (like a metal). The compressive stress/strain curve of such a composite is slightly concave from the origin up to a point of total reversibility. Deforming beyond this point causes irreversible damage to the foamed metal so that the composite has a permanent offset of $\leqslant$ 4% and subsequent loading cycles are associated with a stress/strain curve akin to that of the elastomer by itself, and the volume electrical resistivity becomes much higher. Deforming to levels below this point allows subsequent loading cycles to exhibit a stress/strain curve exactly the same as in the first cycle. Thus, the point of total reversibility is the practical limit for the use of the composite. At the point of total reversibility in the first loading cycle, the stress/strain curve shows a discontinuous change in slope. The shape of the stress/strain curve in the first cycle is different from that of the metal itself as well as that of silicone itself, indicating that the bonding or interaction between the metal and the silicone is appreciable.

The point of total reversibility occurs at a compressive stress of 2 MPa and a strain of 13% for Sn/silicone A, but occurs at a compressive stress of 0.33 MPa and a strain of 0.66% for Sn–Pb/silicone A. This difference between Sn and Sn–Pb is attributed to the less ductile and stiffer nature of Sn–Pb. A further cause of this difference is the poorer bonding between Sn–Pb and silicone compared with that between Sn and silicone, as revealed by metallography and fractography.

Although Sn/silicone is much superior to Sn–Pb/silicone in mechanical properties, it is inferior to Sn–Pb/silicone in the volume electrical resistivity and the contact resistivity (with copper), which are both larger for Sn/silicone than for Sn–Pb/silicone. The higher volume resistivity of Sn/silicone is attributed to the slight physical damage to the tin during the silicone infiltration. The higher contact resistivity of Sn/silicone (with copper) is attributed to the partial removal of the soft tin at the surface of the composite during polishing, as shown by metallography.

The difference between Sn/silicone and Sn–Pb/silicone in electrical properties is small compared with the difference in the mechanical properties. Therefore, overall, Sn/silicone is more attractive than Sn–Pb/silicone for use as a resilient conductor.

Sn–Pb/silicone B is superior to Sn–Pb/silicone A in both the electrical and mechanical properties, although the difference is not large.

Although the thermal conductivity was not measured, it is obvious that the thermal conductivity of the composites is high because of the interconnected nature of the metal in the composites.

An added attraction of the Sn/silicone composite lies in the low thermal expansion coefficient compared with that of silicone. The low thermal expansion makes this composite more compatible with other materials in electronic packaging.

Another attraction of the Sn/silicone composite lies in the low materials and fabrication costs. In contrast, commercially available conducting silicones commonly use expensive silver particles as the conducting phase in the composite.

One disadvantage of Sn/silicone compared with Sn–Pb/silicone is in the poorer fatigue resistance, as shown by the significant increase in the contact resistivity after 900 compressive loading cycles (0.8 MPa). In contrast, for Sn–Pb/silicone, the contact resistivity remains low up to ~ 1400 cycles. Similarly, the volume resistivity of Sn/silicone starts to increase after 300 compressive loading cycles (0.075 MPa), though it remains below 1×10^{-3} Ω cm up to 1700 cycles. These effects are attributed to fretting corrosion, which is common for tin contacts[4]. However, lubricants are available for use with tin contacts to provide stable contact performance beyond 20 000 cycles[4].

CONCLUSIONS

Sn/silicone containing foamed tin amounting to 14 vol % Sn is a new composite material that is resilient up to a compressive stress of 2 MPa and a corresponding strain of 13%. The compressive stress/strain curve is slightly concave up to this limit, below which subsequent loadings follow this same stress/strain curve and above which subsequent loadings follow a concave curve akin to that of silicone by itself.

The Sn/silicone composite exhibits a volume electrical resistivity of 5×10^{-4} Ω cm and the value remains below 1×10^{-3} Ω cm after 1700 compressive loading cycles at 0.075 MPa.

The contact resistivity between the Sn/silicone composite and a copper sheet drops with increasing pressure and levels off at 0.22 Ω cm^2 at a pressure of 0.07 MPa. Thus, a pressure exceeding 0.07 MPa should be applied when the composite is used as an electrical contact with copper.

The contact resistivity between Sn/silicone and copper remains at or below 0.22 Ω cm^2 for compressive loading cycles (0.08 MPa) up to 500 and remains at or below 0.25 Ω cm^2 for loading cycles up to 800 cycles. Beyond 1000 cycles, the contact resistivity rises, reaching a value of 0.48 Ω cm^2 at 1700 cycles.

The thermal expansion coefficient of the Sn/silicone composite is 215×10^{-6}°C^{-1} at 45°C, compared with a corresponding value of 282×10^{-6}°C^{-1} for silicone itself.

Compared with the Sn/silicone composite, Sn–Pb/silicone containing foamed Sn–Pb (37 wt % Pb) amounting to 15 vol % Sn–Pb exhibits a lower volume electrical resistivity, a lower contact resistivity (with copper) and a higher fatigue resistance, but it is resilient only up to a compressive stress of 0.4 MPa and a corresponding strain of 0.8%.

The Sn/silicone composite is technologically attractive as a new material for electrical and thermal contacts in electronic packages.

ACKNOWLEDGEMENTS

The authors are grateful to Daniel G. LaBarge of the State University of New York at Buffalo for technical assistance. They also acknowledge the support of the Center for Electronic and Electro-Optic Materials.

REFERENCES

1 **Davies, G.J. and Zhen, S.** *J Mater Sci* **18** (1983) p 1899
2 **Sinha, S.K. and Rao, G.N.** *NML Tech J* **18** (1976) p 21
3 **Kuchek, H.A.** *US Pat 3 236 706* (1966)
4 **Mroczkowski, R.** *Adv Mater Proc* **134** No 6 (1988) p 49

AUTHORS

The authors are with the Composite Materials Research Laboratory, Furnas Hall, State University of New York at Buffalo, Buffalo, NY 14260, USA. Enquiries should be directed to Dr Chung.